RESEARCH ARTICLE

A novel chronic nerve compression model in the rat

Zhen-Yu Liu, Zhen-Bing Chen*, Jiang-Hai Chen*
Department of Hand Surgery, Union Hospital, Tongji Medical College, Huazhong University of Science and Technology, Wuhan, Hubei Province, China

Funding: *This study was supported by the National Natural Science Foundation of China, No. 81471270.*

Graphical Abstract

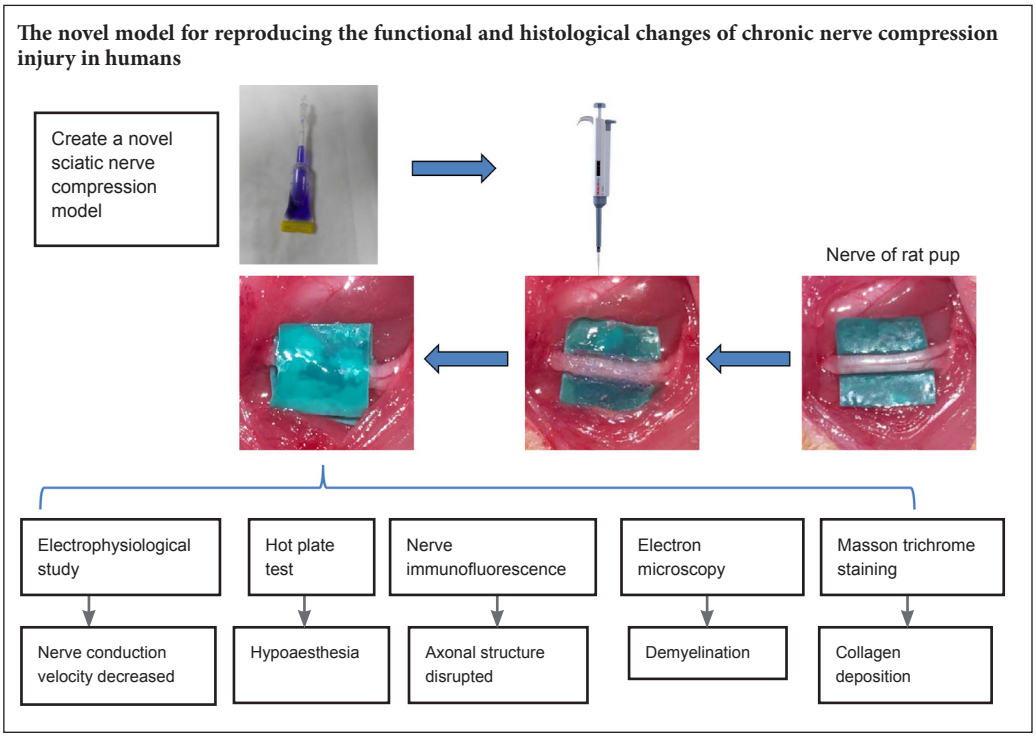

Correspondence to:
Zhen-Bing Chen or Jiang-Hai Chen, 739250311@qq.com or chenjianghai@hust.edu.cn.

orcid:
0000-0001-9712-6854 (Jiang-Hai Chen)

doi: *10.4103/1673-5374.235306*

Accepted: *2018-06-15*

Abstract

Current animal models of chronic peripheral nerve compression are mainly silicone tube models. However, the cross section of the rat sciatic nerve is not a perfect circle, and there are differences in the diameter of the sciatic nerve due to individual differences. The use of a silicone tube with a uniform internal diameter may not provide a reliable and consistent model. We have established a chronic sciatic nerve compression model that can induce demyelination of the sciatic nerve and lead to atrophy of skeletal muscle. In 3-week-old pups and adult rats, the sciatic nerve of the right hind limb was exposed, and a piece of surgical latex glove was gently placed under the nerve. N-butyl-cyanoacrylate was then placed over the nerve, and after it had set, another piece of glove latex was placed on top of the target area and allowed to adhere to the first piece to form a sandwich-like complex. Thus, a chronic sciatic nerve compression model was produced. Control pups with latex or N-butyl-cyanoacrylate were also prepared. Functional changes to nerves were assessed using the hot plate test and electromyography. Immunofluorescence and electron microscopy analyses of the nerves were performed to quantify the degree of neuropathological change. Masson staining was conducted to assess the degree of fibrosis in the gastrocnemius and intrinsic paw muscles. The pup group rats subjected to nerve compression displayed thermal hypoesthesia and a gradual decrease in nerve conduction velocity at 2 weeks after surgery. Neuropathological studies demonstrated that the model caused nerve demyelination and axonal irregularities and triggered collagen deposition in the epineurium and perineurium of the affected nerve at 8 weeks after surgery. The degree of fibrosis in the gastrocnemius and intrinsic paw muscles was significantly increased at 20 weeks after surgery. In conclusion, our novel model can reproduce the functional and histological changes of chronic nerve compression injury that occurs in humans and it will be a useful new tool for investigating the mechanisms underlying chronic nerve compression.

Key Words: *nerve regeneration; chronic nerve compression; carpal tunnel syndrome; nerve conduction velocity; N-butyl-cyanoacrylate; hypoesthesia; demyelination; remyelination; intrinsic muscles; collagen deposition; axonal irregularity; neural regeneration*

Introduction

Chronic nerve compression (CNC) injuries, such as carpal tunnel syndrome, cubital tunnel syndrome, and tarsal tunnel syndrome, are very common (Levine et al., 1993; Papanicolaou et al., 2001; Flanigan and DiGiovanni, 2011). Many complications, such as neuropathic pain, numbness, skeletal muscle atrophy, and motor disability, can result from CNC injury. Much of the current understanding of CNC is derived from studies involving animal models, especially animal models in which the sciatic nerve is banded with Silastic tubing. Mackinnon et al. (1984) described a rodent CNC model in which Silastic tubes with internal diameters ranging from 0.6 mm to 1.5 mm were used to band the sciatic nerve of adult Sprague-Dawley rats. This induced consistent histological changes in the affected nerve over several months. However, tubes with an internal diameter ranging from 0.9 mm to 1.1 mm have a smaller diameter than the nerve (whose mean diameter is 1.3 mm) and, thus, can induce actual physical compression and nerve injury. Furthermore, tubes with an internal diameter of 1.5 mm are likely to induce mechanical stimulation or foreign body reactions in the nerve. O'Brien et al. (1987) banded the sciatic nerve with a tube whose internal diameter was similar to that of the nerve (1.3 mm) and reconstituted the tube with 3 6-0 Prolene sutures. They noted apparent histological changes and slowing of nerve conduction velocity (NCV) at 5 months after surgery. They also noted that long periods of compression caused connective tissue fibrosis and thickening, as well as fibroblast proliferation-induced epineural scarring, resulting in nerve fiber pathology. Decreases in axonal numbers and function were also noted in the late post-injury period. Thus, the histopathological characteristics of chronic compression injury differed from those characterizing Wallerian degeneration, which is precipitated by axonal degeneration. The placement of the sutures as well as the knotting of the sutures may have changed the shape of the tube. Gupta and Steward (2003) recently introduced a new CNC model, a modified version of O'Brien's model, in which a Silastic tube with an internal diameter of 1.3 mm was atraumatically placed on the sciatic nerve (approximately 1–1.1 mm in diameter) without sutures. This model eventually induced chronic nerve injury characterized by local demyelination and remyelination, and phenotypic switching of the neurons within the dorsal root ganglia (Gupta et al., 2004, 2012; Chao et al., 2008). The model mimics the constrained spaces through which normal human peripheral nerves must pass but does not duplicate the increased pressure found at sites of anatomical narrowing.

The tubes used for existing models of compression neuropathy are round and uniform in size. However, nerves are oblate *in vivo* and may have different thicknesses in different individuals. Thus, the above models do not seem to resemble human nerve compression. Moreover, in the clinic, entrapment neuropathy causes sensory dysfunction, muscle weakness and wasting in severe CNC patients. The above animal models have been used to investigate various post-CNC injury-related changes, such as hypoalgesia, local nerve demyelination or cutaneous neurovascular changes (Gupta et al., 2006; Lin et al., 2012; Pelletier et al., 2012). However, none of these studies reported muscle histopathological changes over observational periods of 8 or even 12 months (Mackinnon et al., 1985; O'Brien et al., 1987; Gupta and Steward, 2003). Both the carpal tunnel and the cubital tunnel are well known to be fibro-osseous structures formed by ligaments and bones. These conditions, in which nerves become entrapped by bony and ligamentous structures, cannot be reproduced by the current models. Most CNC injuries encountered in the clinic are caused by gradually worsening compression. Herein, we propose a new technique for inducing CNC. We used pieces of latex glove and N-butyl-cyanoacrylate (NBCA), a tissue adhesive used for nerve repair, to enclose the sciatic nerves of rats (Choi et al., 2004; Elgazzar et al., 2007). We assessed the histological and functional changes induced by the new CNC injury model and verified its validity.

Materials and Methods

Animals

Male Sprague-Dawley rat pups aged 3 weeks and weighing 70–100 g (n = 70) and adult male Sprague-Dawley rats aged 8 weeks and weighing 250–300 g (n = 20) were used. These specific-pathogen-free rats were obtained from the Laboratory Animal Center, Huazhong University of Science and Technology in Wuhan, China (animal license No. SYXK (E) 2016-0057). All surgical and animal care procedures were approved by the Institutional Animal Care and Use Committee at Tongji Medical College, Huazhong University of Science and Technology, China (approval No. 410).

Surgical procedures

All surgical procedures were performed under aseptic conditions. A surgical latex glove (Ansell, Shanghai, China) was cut into small 5 mm × 5 mm pieces. These were immersed overnight in 75% ethanol in a sterilized Petri dish and then washed for 5 minutes three times in sterile water to minimize inflammation. Rats were anesthetized by an intraperitoneal injection of 1% sodium pentobarbital (40 mg/kg). The NBCA compression model was established in 40 pup and 20 adult rats. The sciatic nerve of the right hind limb was exposed through a gluteal-splitting approach, and a piece of latex glove was gently placed under the nerve to ensure that the nerve was not stretched or twisted. Before applying NBCA, the nerve and latex were soaked with fetal bovine serum (Gibco, New York, NY, USA). Using a dissecting microscope (Zeiss, Brunswick, Germany), NBCA (Histoacryl, B.Braun Surgical, Melsungen, Germany) was applied to the nerve in a dropwise manner. All the NBCA was contained by the latex glove material. Approximately 2.5 μL of NBCA was used for each pup, and approximately 5 μL of NBCA was used for each adult. After the NBCA had coagulated, another piece of surgical glove latex was placed on top of the target area and allowed to adhere to the first piece to form a sandwich-like complex (**Figure 1A, B**). To exclude a direct influence of the latex and NBCA on the nerve, two control groups were prepared. In 15 pups, a piece of latex glove was coiled into a tube with an internal diameter of approximately 2 mm so that the nerve would not be compressed during the experiment. The right sciatic nerve was banded with the tube, and these rats served as the latex control group (CON1) (**Figure 1C**). In another 15 pups, the right sciatic nerve was

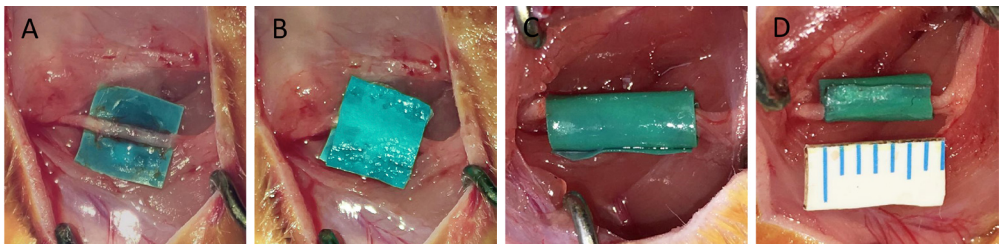

Figure 1 Establishment of the rat chronic nerve compression model.
(A, B) A sandwich-like complex is formed by latex glove pieces and NBCA. (C) Latex pieces control group: The right sciatic nerve is banded with a latex glove tube. (D) NBCA control group: The right sciatic nerve is banded with a latex glove tube whose inner wall is coated with NBCA. NBCA: N-butyl-cyanoacrylate.

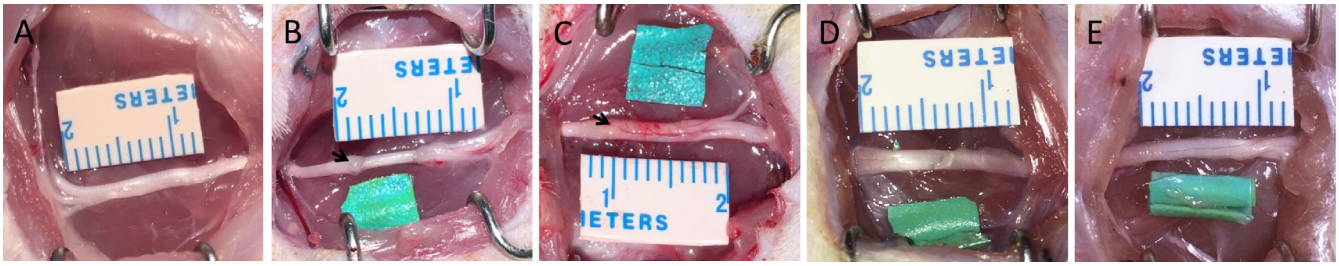

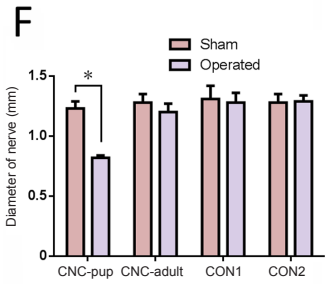

Figure 2 Sciatic nerve after removal of the bundles at 8 weeks post-operation in the novel chronic nerve compression model.
(A) Sciatic nerve in the sham-operated side. (B) Sciatic nerve in the NBCA-treated pup group. (C) Sciatic nerve in the NBCA-treated adult group. (D) Sciatic nerve in the latex pieces pup control group (CON1). (E) Sciatic nerve in the NBCA pup control group (CON2). The arrows indicate swelling of the sciatic nerve. (F) Quantitative results of the average diameter on the mid-point of nerves at the compression site in each group. All data are represented as the mean ± SD (repeated measures one-way analysis of variance followed by Dunnett's *post hoc* test). ∗P < 0.05. Sham: Sham-operated side; operated: experimental side. NBCA: N-butyl-cyanoacrylate; CNC: chronic nerve compression.

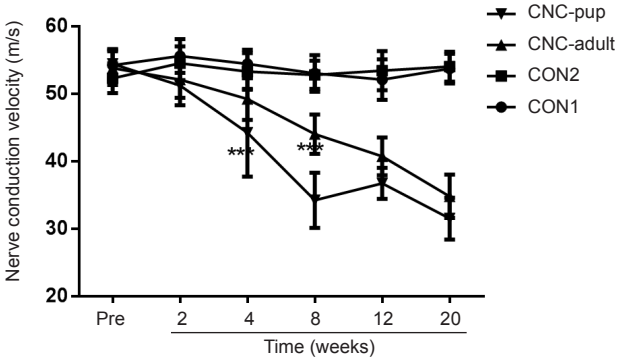

Figure 3 Change of nerve conduction velocity in the novel chronic nerve compression (CNC) model.
Nerve conduction velocity at pre-operation and at each time point post-operation in the N-butyl-cyanoacrylate (NBCA)-treated pup group (CNC-pup) (n = 15), the NBCA-treated adult group (CNC-adult) (n = 5), the latex pieces pup control group (CON1) (n = 3) and the NBCA pup control group (CON2) (n = 3). Compared with pre-operation values, the nerve conduction velocity in the NBCA-treated pup group showed a progressive decline beginning at 4 weeks after the operation; and the NBCA-treated adult group showed a marked decrease at 8 weeks after the operation. All data are represented as the mean ± SD (repeated measures one-way analysis of variance followed by Dunnett's *post hoc* test). ∗∗∗P < 0.001, *vs.* CON1, 2.

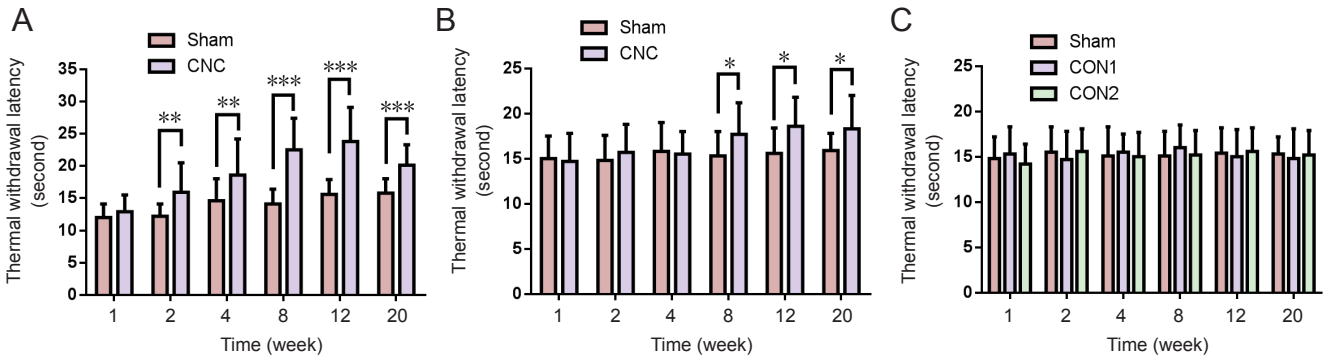

Figure 4 Change in hindpaw withdrawal latency in the novel CNC model in the hotplate test.
(A) Withdrawal latency of the CNC-operated paw was significantly increased following 2 weeks of compression in the NBCA-treated pup group (n = 15). (B) The withdrawal latency of the CNC-operated paw was significantly increased following 8 weeks of compression in the NBCA-treated adult group (n = 5). (C) The withdrawal latency of the latex pieces pup control group (CON1) and the NBCA pup control group (CON2) remained unchanged (n = 3). All data are represented as the mean ± SD (repeated measures one-way analysis of variance followed by Dunnett's *post hoc* test). ∗P < 0.05, ∗∗P < 0.01, ∗∗∗P < 0.001. NBCA: N-butyl-cyanoacrylate; CNC: chronic nerve compression.

banded with a latex glove tube (2 mm internal diameter) whose inner wall was coated with NBCA. These rats served as the NBCA control group (CON2) (**Figure 1D**). The contralateral sciatic nerve of each rat was exposed but was not treated and was replaced within the host muscle bed. This nerve served as a sham-operated control. Each wound was closed with 3-0 polyester sutures upon completion of the procedure. Animals were killed for histological studies by anesthetic overdose (100 mg/kg) of sodium pentobarbital. Sciatic nerves and muscles were harvested from the surgical and nonsurgical sides at different time points after surgery.

Electrophysiological studies
The NCV of the sciatic nerve was measured using an NID-092 electronic medical instrument (Haishen, Shanghai, China) at pre-operation, and at 2, 4, 8, 12 and 20 weeks post-operation. The stimulating electrode was placed on the proximal and distal sides of the compression area of the sciatic nerve (stimulation duration: 0.1 ms; frequency: 1 Hz; stimulus intensity: 5 mA), and the recording electrode was placed on the dorsum of the foot. Latency was evaluated using data obtained directly from the sciatic nerves.

Hotplate test
Sensory studies were conducted at 1, 2, 4, 8, 12 and 20 weeks post-operation. The surface of the hotplate was heated to a maximum temperature of 52.5–53.5°C, and then the rat was placed on the testing apparatus (Yuyan Instruments, Shanghai, China) and a timer was started. The latency to respond to the thermal stimulus applied to the hindpaw was determined by recording the time that elapsed between the point at which the stimulus was applied and that at which the rat licked its hindpaw. The rat was immediately removed from the apparatus once the licking response was observed. If the rat did not respond to the stimulus within 30 seconds, the test was terminated to prevent burns, and the rat was removed from the hotplate (Woolfe, 1944).

Immunofluorescence
At different time points post-surgery (4, 8, 12, and 20 weeks), NBCA-treated nerves from each group were harvested for immunofluorescence. Frozen 10 μm transverse and longitudinal sections of the sciatic nerve were mounted on slides, dried and then immersed in phosphate-buffered saline (PBS) containing 0.3% Triton X-100 for 5 minutes. Sections were then blocked in PBS containing 10% donkey serum for 1 hour at 37°C. Transverse sections were subsequently incubated with mouse monoclonal anti-neurofilament (NF) 200 antibody (1:200 dilution; Abcam) overnight at 4°C. Longitudinal sections were incubated with rabbit anti-collagen I monoclonal antibody (1:200; Abcam) overnight at 4°C. The sections were then washed three times in PBS before being incubated with the appropriate secondary antibody (donkey anti-mouse Alexa-Fluor 488 or donkey anti-rabbit Alexa-Fluor 594) for 1 hour at 37°C. Nuclei were counterstained with 4′6-diamidino-2-phenylindole (DAPI) for 5 minutes (1:500; Sigma). The slides were then washed for 5 minutes three times in PBS (pH 7.4) and coverslips mounted with Fluoromount (Abcam). The primary antibody was omitted in the negative control samples. The sections were visualized using a confocal laser scanning microscope (TCS-SP5; Leica, Mannheim, Germany). The percentage of the transverse nerve section that stained positive for NF and the collagen volume fraction in the sciatic nerve (excluding the epineurium) were evaluated using Image-Pro Plus 6.0 image analysis software (Media Cybernetics, Rockville, MD, USA). To prevent observer bias, the slides were randomly numbered. Moreover, the slides were interpreted in a blinded manner, and each slide was assessed by three observers.

Transmission electron microscopy
To evaluate myelin sheath changes, nerve samples were evaluated *via* standard transmission electron microscopy analysis at 8, 12, and 20 weeks post-operation. Nerve samples were embedded for transverse section analysis. The sections were assessed qualitatively with an Eclipse E800 upright compound microscope (Nikon, Tokyo, Japan) equipped with a Spot camera using an oil immersion Plan Fluor 3100/1.3 N.A. objective lens. Ultrathin sections were imaged using a JEOL JEM 1230 transmission electron microscope. Myelin thickness was measured using ImageJ software (National Institutes of Health, USA). Only myelin regions exhibiting no signs of non-compaction and featuring no fixation artifacts were included in the analysis.

Masson trichrome staining
Tissue samples from both sides of the gastrocnemius muscle and the intrinsic muscles of the hindpaw were harvested at 20 weeks post-surgery. The samples were embedded in paraffin and 5-μm-thick sections prepared. Five slides of each sample were randomly selected for Masson trichrome staining, which was performed according to the manufacturer's protocol (Masson's Trichrome Staining Kit; Boster, Wuhan, China). Sections were evaluated at 100× and 400× magnification to assess collagen fiber size, shape, and distribution. Five fields in each slide were randomly chosen and photographed at 400× magnification and then analyzed to determine the average collagen volume fraction of muscle fibers using Image-Pro Plus 6.0 image analysis software (Media Cybernetics, Rockville, MD, USA) (collagen volume fraction % = collagen area/total cross-sectional area × 100%).

Statistical analysis
The data are presented as the mean ± SD. Statistical significance was analyzed by repeated measures one-way analysis of variance. Dunnett's *post hoc* test was used for multiple comparisons. Statistical analyses were performed using SPSS 16.0 software (SPSS, Chicago, IL, USA). A P-value < 0.05 was considered statistically significant.

Results

Appearance of the sciatic nerve in the novel CNC model
The sciatic nerve was not adhered to the NBCA complex at 3 days post-operation. The nerve could be easily separated from the complex when the latex pieces were longitudinally cut along the nerve. The diameter of the compressed nerve was significantly smaller than that of the contralateral nerve (P < 0.05) and swelling was present distal and proximal to the site treated with NBCA in the NBCA-treated pup group (**Figure 2B**). The width of the proximal and distal nerve

was measured from a photograph using ImageJ analysis software before the nerve was harvested. The average width of the nerve at the compression site was approximately 0.8 mm, while the average width of the contralateral nerve was approximately 1.2 mm. The adult NBCA rats were found to have slight swelling in the segments proximal and distal to the site of nerve compression. The width of the nerve at the compression site was similar to that of the contralateral nerve (**Figure 2C**). No significant difference in nerve width was evident between the two control groups.

NCV decreased in the novel CNC model

Electrophysiological analysis of the NBCA-treated pups (n = 15) showed that the NCV of the compressed nerve was relatively stable until 4 weeks post-operation ($P < 0.001$) compared with pre-operation values and those of the control group. The NCV then decreased gradually and reached 59% of the pre-operation values at 20 weeks post-operation. In NBCA-treated adults (n = 5), there was a considerable decrease in the NCV until 8 weeks post-operation. The NCV then gradually decreased for 20 weeks. No significant difference in the NCV was observed between the two control groups (n = 3; **Figure 3**).

Thermal withdrawal latency increased in the novel CNC model

The hotplate test was performed to evaluate the sensitivity of the CNC-injured limbs. In pups, NBCA-treated limbs (n = 15) displayed similar paw withdrawal latencies to those of the contralateral limbs at 1 week after CNC injury. However, the hindpaw withdrawal latencies of the compressed limbs were significantly longer than those of the contralateral limbs at 2 weeks post-surgery ($P < 0.01$), indicating that the NBCA-treated pups had developed hypoesthesia of the hindpaw at this time point. Similar results were noted at 8 to 20 weeks post-operation. We noted increases in the thermal threshold latency in the contralateral paw between 2 and 20 weeks post-surgery, which we attributed to age-related changes (Hess et al., 1981; Ririe et al., 2003). In the NBCA-treated adult group (n = 5), the hindpaw withdrawal latencies of the compressed limbs did not change until 8 weeks post-surgery. The latency increased significantly ($P < 0.05$) compared with that in the contralateral paw at 8, 12, and 20 weeks post-surgery (**Figure 4B**). No significant changes were found in the two control groups (n = 3; **Figure 4C**).

Collagen deposition in sciatic nerves of the novel CNC model

At 8 weeks post-compression, the entrapped and contralateral sciatic nerves of each group were analyzed to assess the degree of collagen deposition. In the NBCA-treated pup group (n = 5), immunofluorescence revealed that collagen I was present in both the margin and the center of the compressed nerve. The collagen volume fractions of the compressed sciatic nerves were significantly higher than those of the contralateral nerves ($P < 0.001$). In addition, collagen I was highly expressed in areas proximal to the compressed region. Intense linear or spotted collagen staining indicated that the perineurium in the corresponding region had thickened. Intense collagen staining was present mainly in the epineurium of the compressed nerve. Collagen staining in the intact nerve was relatively weak (**Figure 5**). We also noted collagen deposition in the epineurium and perineurium of the compressed nerve in the NBCA-treated adults (n = 5). The collagen volume fractions were higher than those of the contralateral nerves ($P < 0.001$) but were lower than those of the pup group ($P < 0.001$). We noted collagen deposition in the epineurium but not in the perineurium in the two control groups (n = 3; **Figure 5**). The collagen volume fractions were 0.640 ± 0.028% in control group 1 and 0.553 ± 0.036% in control group 2 ($P > 0.05$).

To investigate axonal changes induced by CNC injury, transverse sections of the compressed sciatic nerve were immunostained for NF. Immunofluorescence showed that the NF expression pattern in the compressed nerve was more irregular than in the contralateral nerve of the NBCA-treated pups at different time points (n = 20; **Figure 6A**), indicating that the axonal structure of the compressed nerve was disrupted. Dense staining of the outermost nuclei suggested that the cells constituting the epineurium had proliferated, resulting in epineural thickening. The percentage of the total transverse sectional area that was stained positive for NF in the compressed nerve was significantly lower than that in the intact nerve beginning at 8 weeks post-operation ($P < 0.05$; **Figures 6B–E**). Immunofluorescence showed that the axonal structure of the compressed nerve was slightly disordered in the NBCA-treated adults (n = 20) beginning at 8 weeks post-operation. However, the degree to which the axonal structure was disrupted did not increase until 20 weeks post-surgery (**Figures 6F–I**).

Myelin thickness of sciatic nerves in the novel CNC model

Electron microscopy evaluation showed compression induced changes in the myelin sheath. We noted separation of the myelin lamellae, swelling, and vacuolization in NBCA-treated pups, and the average thickness of the sheath in the affected nerve decreased to a value that was 63% of that in the contralateral nerve ($P < 0.001$) at 8 weeks after surgery. This disorganization continued up to 12 weeks after compression because the sheath was thinner at 12 weeks post-compression than at 8 weeks post-compression. However, the thickness of the myelin sheath was increased at 20 weeks after compression compared with 12 weeks after compression ($P < 0.001$) and was not comparable with that of the intact sheath (**Figures 7A–F**). The average myelin sheath thickness in the compressed nerve in the NBCA-treated adults was 68% of that in the contralateral nerve at 8 weeks post-compression ($P < 0.001$) and decreased to a value that was 59% of that in the contralateral nerve at 20 weeks post-compression (**Figures 7G–L**).

Collagen fibers in the gastrocnemius muscle and the intrinsic muscles of the hindpaw in the novel CNC model

Muscle morphology in the NBCA-treated pups (n = 5) was observed by Masson staining. The collagen volume fractions of the CNC gastrocnemius muscle were significantly higher than those of the contralateral muscles ($P < 0.001$). Furthermore, the collagen volume fractions of the intrinsic muscles of the hindpaw were significantly higher than those of the contralateral muscles (**Figure 8**). No significant increases in collagen deposition in the gastrocnemius muscle and the

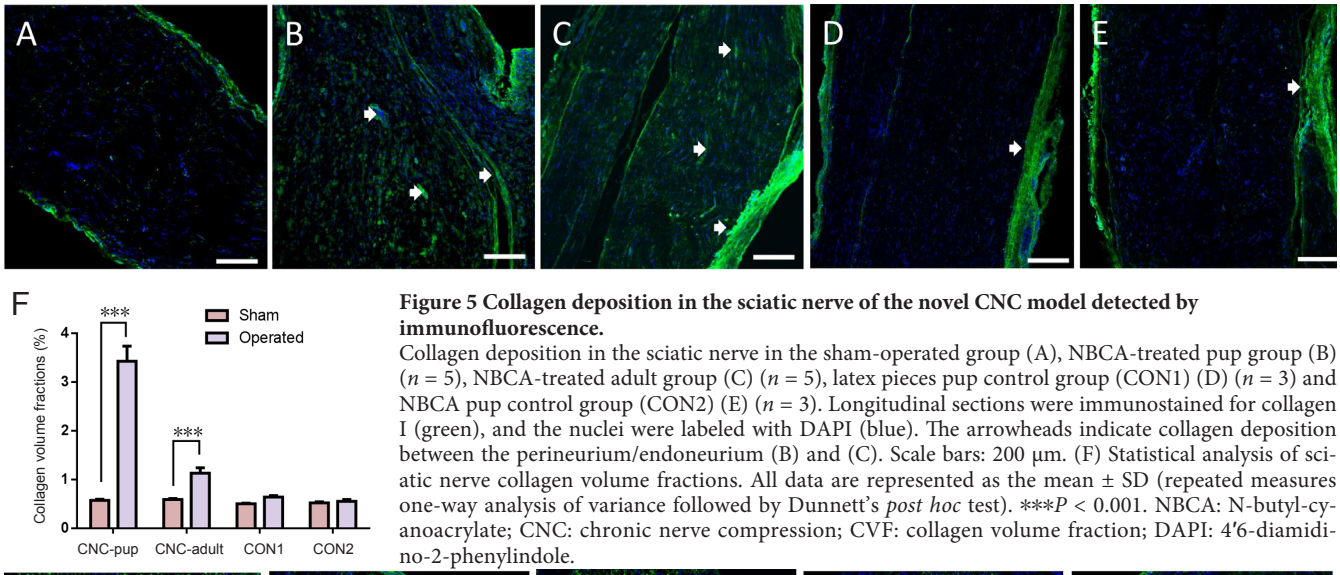

Figure 5 Collagen deposition in the sciatic nerve of the novel CNC model detected by immunofluorescence.
Collagen deposition in the sciatic nerve in the sham-operated group (A), NBCA-treated pup group (B) (n = 5), NBCA-treated adult group (C) (n = 5), latex pieces pup control group (CON1) (D) (n = 3) and NBCA pup control group (CON2) (E) (n = 3). Longitudinal sections were immunostained for collagen I (green), and the nuclei were labeled with DAPI (blue). The arrowheads indicate collagen deposition between the perineurium/endoneurium (B) and (C). Scale bars: 200 μm. (F) Statistical analysis of sciatic nerve collagen volume fractions. All data are represented as the mean ± SD (repeated measures one-way analysis of variance followed by Dunnett's *post hoc* test). ***P < 0.001. NBCA: N-butyl-cyanoacrylate; CNC: chronic nerve compression; CVF: collagen volume fraction; DAPI: 4′6-diamidino-2-phenylindole.

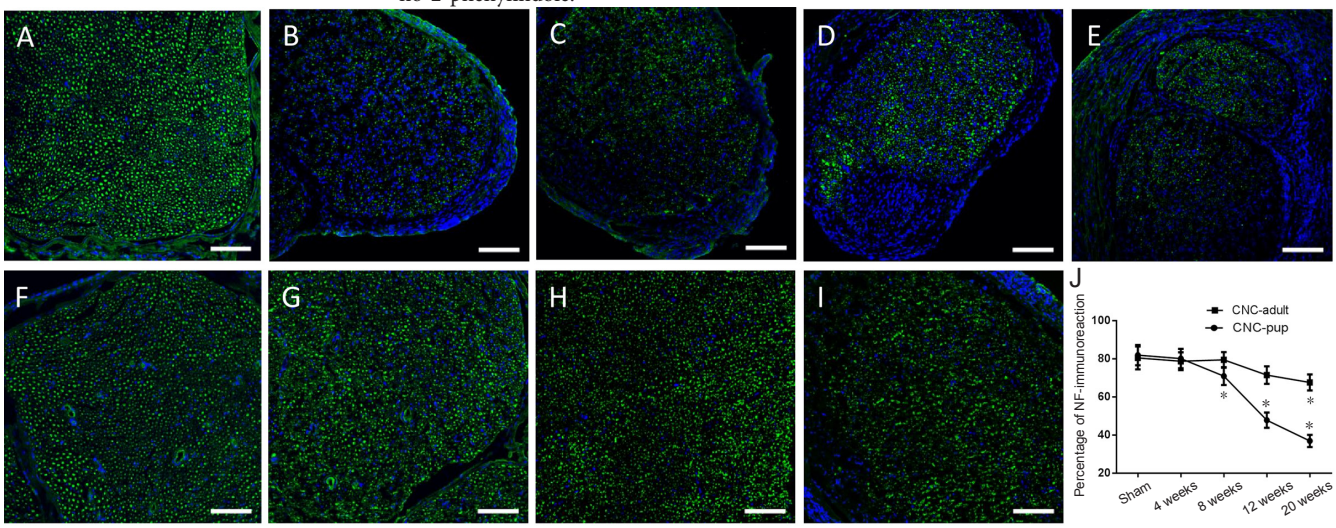

Figure 6 Immunofluorescence staining of NF in sciatic nerves of the novel CNC model.
Cross sections are immunostained for NF-200 (green), and nuclei are labeled with DAPI (blue). (A) Sham-operated nerve. Immunostaining for NF-200 in compressed sciatic nerves at 4, 8, 12 and 20 weeks post-operation in the NBCA-treated pup group (n = 20) (B–E) and NBCA-treated adult group (n = 20) (F–I), respectively. Scale bars: 100 μm. (J) Quantification of the percentage of NF-immunoreactivity in sciatic nerves. All data are represented as the mean ± SD (repeated measures one-way analysis of variance followed by Dunnett's *post hoc* test). *P < 0.05, *vs.* sham. NBCA: N-butyl-cyanoacrylate; CNC: chronic nerve compression; NF: neurofilament; DAPI: 4′6-diamidino-2-phenylindole.

intrinsic muscles of the hindpaw were detected at 20 weeks post-operation in the NBCA-treated adults (n = 5; **Figure 8**) or in the two control groups (data not shown).

These results demonstrated that the novel CNC model induced symptoms similar to those associated with CNC in humans.

Discussion

CNC injury is a common clinical problem that often results in significant morbidity, including loss of motor and sensory functions. CNC injury may cause amyotrophy, paresthesia, and paralysis (Thonnard et al., 1999; Tamburin et al., 2008). The pathological changes and mechanisms underlying these conditions remain to be elucidated. To date, published CNC animal models only partially reproduce the pathological characteristics of human CNC injury, which often occurs in response to soft tissue compression by semi-solid surfaces. The present study established a new CNC rat model. We found that applying NBCA to the sciatic nerve and using a piece of latex glove to band the nerve led to sensory dysfunction and muscle changes. In this model, the NBCA and latex glove form a semi-solid and semi-soft structure similar to that of the human nerve canal. Previous studies have suggested that NBCA is nontoxic to nerve tissues and can be used as an alternative treatment in peripheral nerve repair (Landegren et al., 2006; Elgazzar et al., 2007; Papalia et al., 2016). Choi et al. (2004) noted good axonal regeneration and a mild foreign body reaction around cyanoacrylates when a microdrop of butyl-2-cyanoacrylate was applied to the surface of the overlapping epineurium. These results are similar to those of the present study. The results for control group 2 indicated that applying NBCA to the surface of the epineurium did not lead to progressive fibrous tissue thickening or local nerve compression. The results for control group 1

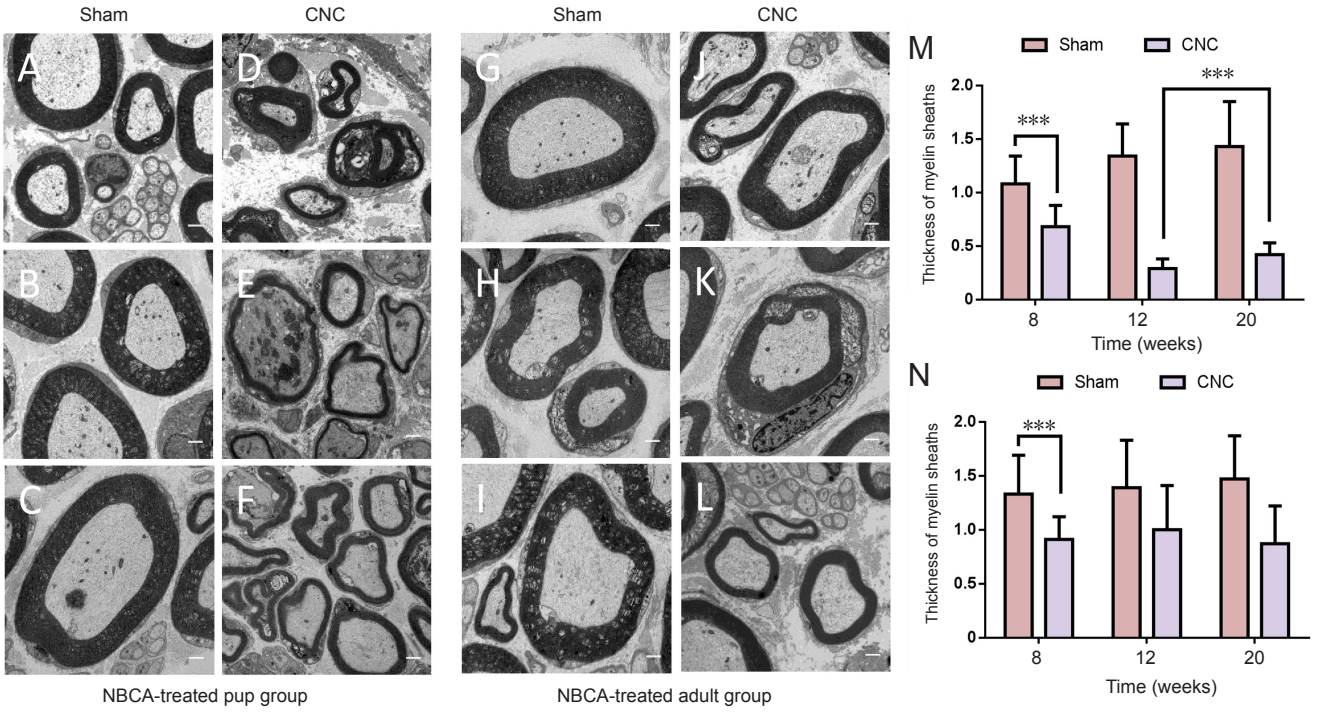

Figure 7 Electron microscopy analysis of sciatic nerves in the novel CNC model.
Electron micrographs of sciatic nerves at the compression site at 8, 12 and 20 weeks post-operation. (A–C) Sham-operated nerves, and (D–F) compressed nerves at 8, 12, and 20 weeks post-operation in the NBCA-treated pup group (n = 15). (G–I) Sham-operated nerves, and (J–L) compressed nerves at 8, 12, and 20 weeks post-operation in the NBCA-treated adult group (n = 15). Scale bars: 1 μm. (M, N) Quantification of the thickness of myelin sheaths in the NBCA-treated pup (M) and adult (N) groups. All data are represented as the mean ± SD (repeated measures one-way analysis of variance followed by Dunnett's *post hoc* test). ***P < 0.001. NBCA: N-butyl-cyanoacrylate; CNC: chronic nerve compression.

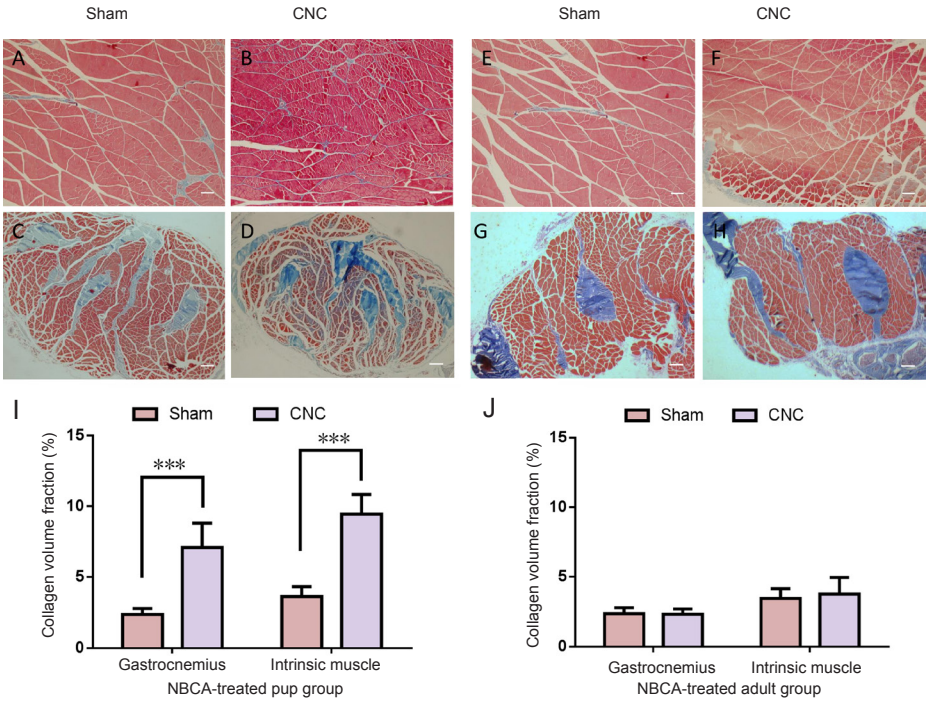

Figure 8 Light microscopy analysis of the gastrocnemius and intrinsic muscles.
Light microscopy images of transverse sectioned muscle samples from the NBCA-pup and NBCA-adult groups following Masson's trichrome staining at 20 weeks after surgery. (A, B) Gastrocnemius and (C, D) intrinsic muscles of the hindpaw in the NBCA-treated pup group (n = 5). (E, F) Gastrocnemius and (G, H) intrinsic muscles of the hindpaw in the NBCA-treated adult group (n = 5). Scale bars: 100 μm. (I, J) Quantitative analyses of collagen volume fraction in the muscles on the sham-operated side and on the chronic nerve compression (CNC) side are presented for the pup (I) and adult (J) groups. All data are represented as the mean ± SD (repeated measures one-way analysis of variance followed by Dunnett's *post hoc* test). ***P < 0.001. NBCA: N-butyl-cyanoacrylate.

indicated that latex pieces did not change nerve histology or local nerve compression. Moreover, this CNC model was only marginally effective in the NBCA-treated adult group. Therefore, the sciatic nerve compression induced by this model is dependent on the growth forces on the nerve as the rat matures as opposed to a foreign body reaction affecting the nerve. In the 3-week-old pups, the sciatic nerve was limited to a fixed space, but as the nerve got thicker with age it gradually became compressed.

Similar to other CNC models, this model showed decreases in NCV and average myelin sheath thickness. Electrophysiological changes occurred at an earlier time point (4 weeks post-operation) in pups in this model than in other models (12 weeks post-operation) (O'Brien et al., 1987; Gup-

ta and Steward, 2003). However, the absence of a change in NCV at 2 weeks post-operation indicated that the compression injury induced in the new model was chronic rather than acute. The hotplate test showed that the withdrawal latency increased in CNC rats compared with control rats, indicating that neuropathic hypoesthesia developed after CNC injury. Hypoalgesia has also been observed in other CNC models (Gupta et al., 2006; Barac et al., 2013) in contrast to the hypersensitivity that is observed with models of neuropathic pain, such as chronic constriction injury (Bennett and Xie, 1988), partial sciatic nerve ligation (Seltzer et al., 1990) and spared nerve injury (Richner et al., 2011) models. In the clinic, patients with nerve compression often complain of allodynia and paresthesia. The mechanism of neuropathic pain is not clear. However, according to our clinical experience, pain is not a classical symptom in CNC patients, although numbness and electric shock-like pain are so intense that they are described as painful. In addition, quantitative sensory testing has revealed thermal hypoesthesia in carpal tunnel syndrome patients (Tamburin et al., 2011; Schmid et al., 2014). In our new model, an initial increase in the ipsilateral thermal withdrawal latency appeared (2 weeks after surgery). Similar findings have been found in humans who have developed entrapment neuropathies. Paresthesia often develops earlier than electrophysiological abnormalities.

In contrast to other studies (Mackinnon and Dellon, 1986; Dellon and Mackinnon, 1991; Aanonsen et al., 1992), the entrapped nerve was thinner than the intact nerve in this study. The rats in the pup group displayed signs of muscle atrophy. Patients who suffer from compressive neuropathies often present with weakness or muscle atrophy in the late stage of the disease (Nora et al., 2004; Mallette et al., 2007). Moreover, collagen deposition was detected in the gastrocnemius muscle and intrinsic muscles of the hindpaw in these rats. The collagen volume fraction of the ipsilateral muscles was higher than that of the contralateral muscles. These results indicate that the new model can induce muscle atrophy. Muscle atrophy has not been noted in previous CNC models. Decreases in axon numbers and axonal degeneration have been detected in previous studies; however, no changes in muscle fiber type or muscle morphology have been observed in existing models employing Silastic tube-induced CNC injury (Mackinnon et al., 1984; O'Brien et al., 1987; Gupta et al., 2004, 2006). Our new model is a significant improvement over previous models, as it enables the study of nerve entrapment-induced muscle atrophy. The above phenomena observed in our model are similar to the clinical symptoms and pathological characteristics of human diseases caused by chronic peripheral nerve compression, such as carpal tunnel syndrome (Han et al., 2011; Floranda and Jacobs, 2013; Kleopa, 2015).

The adult rat group was included in the study not only to demonstrate that the NBCA and latex glove procedure would not lead to immediate compression but also to mimic popular Silastic tube CNC models (O'Brien et al., 1987; Gupta and Steward, 2003). The NBCA model produced similar results in adult rats to those of other models. Specifically, the model induced decreases in NCV, local demyelination, and hypoesthesia in adult rats. The NBCA envelops the nerve very well and is not affected by differences in nerve diameter among rats. We believe that our new model is an improvement over existing models. Moreover, the Silastic tube model, including the model in which the Silastic tube is reinforced with sutures (O'Brien et al., 1987) and that in which only the tube is used (Gupta and Steward, 2003), requires an operation that may be dangerous to the nerve because the Silastic tube must be cut longitudinally and then placed around the nerve. This longitudinal slit created in the tube could cause the nerve to be crushed when the tube is placed around it.

Aguayo et al. (1971) studied chronic progressive nerve injury in young rabbits. These authors placed a large Silastic tube around the sciatic nerve of 3–5-week-old rabbits and placed a suture in the tube. These authors used young animals; thus, the nerve had some space in which to grow and gradually adapt to the compression, which does not occur in human diseases. Moreover, the Silastic tube is round and not a semi-solid and semi-soft structure and, therefore, does not accurately resemble the human nerve canal. Although carpal tunnel syndrome in children is uncommon and most childhood carpal tunnel syndrome is a secondary phenomenon to conditions such as mucopolysaccharidosis, obesity and Cavanagh syndrome (Van Meir and De Smet, 2003; Potulska-Chromik et al., 2014), these diseases increase pressure in the carpal tunnel and eventually cause median nerve compression. These patients or their parents reported improvement either in symptoms or hand function after carpal tunnel release (Yuen et al., 2007). Therefore, the young rats used in this study provide a good nerve compression model of carpal tunnel syndrome in children. In addition, the sciatic nerve was not adhered to the NBCA complex at 3 days post-operation.

In our preliminary experiments, approximately 25% of the NBCA-treated pups were discarded. Their gait changed within 1–2 days after surgery. We found that dry latex deformed when NBCA was deposited directly onto it or onto latex wetted with PBS. However, the latex remained flat when NBCA was deposited onto latex pieces previously soaked in fetal bovine serum. We suspect that the above deformation of the latex results in acute sciatic nerve compression. We, therefore, used the latter method to prevent acute nerve compression. In addition, the fetal bovine serum on the surface of the sciatic nerve prevents long-term adhesion of the NBCA and contributes to the early separation of the nerve and NBCA.

The myelin thickness was recovered by 20 weeks post-operation. Demyelination and remyelination co-exist during CNC. At early time points when the nerve is undergoing fast growth, demyelination is active. As the nerve stops growing and remyelination proceeds, the nerve may repair the injury. Although the novel CNC model might not induce continuous deterioration, it causes chronic muscle dysfunction. However, the compression force does not increase continuously. When the nerves stop growing, the force no longer increases. What occurs when the nerve stops growing and whether dysfunction improves in the late stages of the novel CNC model requires further investigation.

In summary, we have established a novel CNC injury model that simulated both neuropathy and dominant muscle injury. This model may be useful as a new tool for investigating the mechanisms underlying CNC. In addition, the new CNC injury model reproduces the pathological changes of CNC injury in humans.

Author contributions: *ZBC and JHC conceived and designed the study and reviewed and edited the paper. ZYL performed the experiments and wrote the paper. All authors contributed to and have approved the final version of the paper.*
Conflicts of interest: *The authors declare that they have no conflicts of interest or financial disclosures to report.*
Financial support: *This study was supported by the National Natural Science Foundation of China, No. 81471270. The funder had no role in the study design, data collection and analysis, decision to publish, or preparation of the manuscript.*
Institutional review board statement: *The study was approved by the Institutional Animal Care and Use Committee at Tongji Medical College, Huazhong University of Science and Technology, China (approval No. 410).*

Data sharing statement: *Datasets analyzed during the current study are available from the corresponding author on reasonable request.*
Plagiarism check: *Checked twice by iThenticate.*
Peer review: *Externally peer reviewed.*

Open peer reviewer: *Aldo Calliari, Universidad de la República de Uruguay, Uruguay.*
Additional file: *Open peer review report 1.*

References

Aanonsen LM, Kajander KC, Bennett GJ, Seybold VS (1992) Autoradiographic analysis of 125I-substance P binding in rat spinal cord following chronic constriction injury of the sciatic nerve. Brain Res 596:259-268.
Aguayo A, Nair CP, Midgley R (1971) Experimental progressive compression neuropathy in the rabbit. Histologic and electrophysiologic studies. Arch Neurol 24:358-364.
Barac S, Jiga LP, Barac B, Hoinoiu T, Dellon AL, Ionac M (2013) Hindpaw withdrawal from a painful thermal stimulus after sciatic nerve compression and decompression in the diabetic rat. J Reconstr Microsurg 29:63-66.
Bennett GJ, Xie YK (1988) A peripheral mononeuropathy in rat that produces disorders of pain sensation like those seen in man. Pain 33:87-107.
Chao T, Pham K, Steward O, Gupta R (2008) Chronic nerve compression injury induces a phenotypic switch of neurons within the dorsal root ganglia. J Comp Neurol 506:180-193.
Choi BH, Kim BY, Huh JY, Lee SH, Zhu SJ, Jung JH, Cho BP (2004) Microneural anastomosis using cyanoacrylate adhesives. Int J Oral Maxillofac Surg 33:777-780.
Dellon AL, Mackinnon SE (1991) Chronic nerve compression model for the double crush hypothesis. Ann Plast Surg 26:259-264.
Elgazzar RF, Abdulmajeed I, Mutabbakani M (2007) Cyanoacrylate glue versus suture in peripheral nerve reanastomosis. Oral Surg Oral Med Oral Pathol Oral Radiol Endod 104:465-472.
Flanigan RM, DiGiovanni BF (2011) Peripheral nerve entrapments of the lower leg, ankle, and foot. Foot Ankle Clin 16:255-274.
Floranda EE, Jacobs BC (2013) Evaluation and treatment of upper extremity nerve entrapment syndromes. Prim Care 40:925-943, ix.
Gupta R, Steward O (2003) Chronic nerve compression induces concurrent apoptosis and proliferation of Schwann cells. J Comp Neurol 461:174-186.
Gupta R, Rowshan K, Chao T, Mozaffar T, Steward O (2004) Chronic nerve compression induces local demyelination and remyelination in a rat model of carpal tunnel syndrome. Exp Neurol 187:500-508.
Gupta R, Nassiri N, Hazel A, Bathen M, Mozaffar T (2012) Chronic nerve compression alters Schwann cell myelin architecture in a murine model. Muscle Nerve 45:231-241.
Gupta R, Rummler LS, Palispis W, Truong L, Chao T, Rowshan K, Mozaffar T, Steward O (2006) Local down-regulation of myelin-associated glycoprotein permits axonal sprouting with chronic nerve compression injury. Exp Neurol 200:418-429.
Han SE, Lin CS, Boland RA, Kiernan MC (2011) Nerve compression, membrane excitability, and symptoms of carpal tunnel syndrome. Muscle Nerve 44:402-409.
Hess GD, Joseph JA, Roth GS (1981) Effect of age on sensitivity to pain and brain opiate receptors. Neurobiol Aging 2:49-55.
Kleopa KA (2015) In the Clinic. Carpal Tunnel Syndrome. Ann Intern Med 163:ITC1.
Landegren T, Risling M, Brage A, Persson JK (2006) Long-term results of peripheral nerve repair: a comparison of nerve anastomosis with ethyl-cyanoacrylate and epineural sutures. Scand J Plast Reconstr Surg Hand Surg 40:65-72.
Levine DW, Simmons BP, Koris MJ, Daltroy LH, Hohl GG, Fossel AH, Katz JN (1993) A self-administered questionnaire for the assessment of severity of symptoms and functional status in carpal tunnel syndrome. J Bone Joint Surg Am 75:1585-1592.
Lin MY, Frieboes LS, Forootan M, Palispis WA, Mozaffar T, Jafari M, Steward O, Gall CM, Gupta R (2012) Biophysical stimulation induces demyelination via an integrin-dependent mechanism. Ann Neurol 72:112-123.
Mackinnon SE, Dellon AL (1986) Experimental study of chronic nerve compression. Clinical implications. Hand Clin 2:639-650.
Mackinnon SE, Dellon AL, Hudson AR, Hunter DA (1984) Chronic nerve compression--an experimental model in the rat. Ann Plast Surg 13:112-120.
Mackinnon SE, Dellon AL, Hudson AR, Hunter DA (1985) A primate model for chronic nerve compression. J Reconstr Microsurg 1:185-195.
Mallette P, Zhao M, Zurakowski D, Ring D (2007) Muscle atrophy at diagnosis of carpal and cubital tunnel syndrome. J Hand Surg Am 32:855-858.
Nora DB, Becker J, Ehlers JA, Gomes I (2004) Clinical features of 1039 patients with neurophysiological diagnosis of carpal tunnel syndrome. Clin Neurol Neurosurg 107:64-69.
O'Brien JP, Mackinnon SE, MacLean AR, Hudson AR, Dellon AL, Hunter DA (1987) A model of chronic nerve compression in the rat. Ann Plast Surg 19:430-435.
Papalia I, Magaudda L, Righi M, Ronchi G, Viano N, Geuna S, Colonna MR (2016) Epineurial window is more efficient in attracting axons than simple coaptation in a sutureless (cyanoacrylate-bound) model of end-to-side nerve repair in the rat upper limb: functional and morphometric evidences and review of the literature. PLoS One 11:e0148443.
Papanicolaou GD, McCabe SJ, Firrell J (2001) The prevalence and characteristics of nerve compression symptoms in the general population. J Hand Surg Am 26:460-466.
Pelletier J, Fromy B, Morel G, Roquelaure Y, Saumet JL, Sigaudo-Roussel D (2012) Chronic sciatic nerve injury impairs the local cutaneous neurovascular interaction in rats. Pain 153:149-157.
Potulska-Chromik A, Lipowska M, Gawel M, Ryniewicz B, Maj E, Kostera-Pruszczyk A (2014) Carpal tunnel syndrome in children. J Child Neurol 29:227-231.
Richner M, Bjerrum OJ, Nykjaer A, Vaegter CB (2011) The spared nerve injury (SNI) model of induced mechanical allodynia in mice. J Vis Exp:3092.
Ririe DG, Vernon TL, Tobin JR, Eisenach JC (2003) Age-dependent responses to thermal hyperalgesia and mechanical allodynia in a rat model of acute postoperative pain. Anesthesiology 99:443-448.
Schmid AB, Bland JDP, Bhat MA, Bennett DLH (2014) The relationship of nerve fibre pathology to sensory function in entrapment neuropathy. Brain 137:3186-3199.
Seltzer Z, Dubner R, Shir Y (1990) A novel behavioral model of neuropathic pain disorders produced in rats by partial sciatic nerve injury. Pain 43:205-218.
Tamburin S, Cacciatori C, Marani S, Zanette G (2008) Pain and motor function in carpal tunnel syndrome: a clinical, neurophysiological and psychophysical study. J Neurol 255:1636-1643.
Tamburin S, Cacciatori C, Praitano ML, Cazzarolli C, Foscato C, Fiaschi A, Zanette G (2011) Median nerve small- and large-fiber damage in carpal tunnel syndrome: a quantitative sensory testing study. J Pain 12:205-212.
Thonnard J, Saels P, Van den Bergh P, Lejeune T (1999) Effects of chronic median nerve compression at the wrist on sensation and manual skills. Exp Brain Res 128:61-64.
Van Meir N, De Smet L (2003) Carpal tunnel syndrome in children. Acta Orthop Belg 69:387-395.
Woolfe G (1944) The evaluation of the analgesic action of pethidine hydrochloride (Demerol). J pharmacol Exp Ther 80:300-307.
Yuen A, Dowling G, Johnstone B, Kornberg A, Coombs C (2007) Carpal tunnel syndrome in children with mucopolysaccaridoses. J Child Neurol 22:260-263.

(*Copyedited by Yu J, Li CH, Qiu Y, Song LP, Zhao M*)